Well-Defined Colloidal 2-D Layered Transition-Metal Chalcogenide Nanocrystals via Generalized Synthetic Protocols

Sohee Jeong,[†] Dongwon Yoo,[†] Jung-tak Jang, Minkyoung Kim, and Jinwoo Cheon*

Department of Chemistry, Yonsei University, Seoul 120−749, Korea

Ⓢ *Supporting Information*

ABSTRACT: While interesting and unprecedented material characteristics of two dimensionality (2-D) layered nanomaterials are emerging, their reliable synthetic methodologies are not well developed. In this study we demonstrate general applicability of synthetic protocols to a wide range of colloidal 2-D layered transition-metal chalcogenide (TMC) nanocrystals. As distinctly different from other nanocrystals, we discovered that 2-D layered TMC nanocrystals are unstable in the presence of reactive radicals from elemental chalcogen during the crystal formation. We first introduce the synthesis of titanium sulfide and selenide where well-defined single crystallinity and lateral size controllability are verified, and then such synthetic protocols are extended to all of group IV and V transition-metal sulfide (TiS_2, ZrS_2, HfS_2, VS_2, NbS_2, and TaS_2) and selenide ($TiSe_2$, $ZrSe_3$, $HfSe_3$, VSe_2, $NbSe_2$, and $TaSe_2$) nanocrystals. The use of appropriate chalcogen source is found to be critical for the successful synthesis of 2-D layered TMC nanocrystals. CS_2 is an efficient chalcogen precursor for metal sulfide nanocrystals, whereas elemental Se is appropriate for metal selenide nanocrystals. We briefly discuss the effects of reactive radical characteristics of elemental S and Se on the formation of 2-D layered TMC nanocrystals.

In nanoscale regime, dimensionality is one of the critical parameters to modulate physical and chemical properties of nanomaterials.[1] Until now, most research on dimensionality controlled studies has been concentrated on the zero dimensional (0-D) spheres and one-dimensional (1-D) rods and wires.[2] Two dimensionality (2-D) in nanomaterials is emerging fast, exhibiting unexpected new phenomena which are absent from other dimensionality.[3] Beyond studies of graphene, newly rising interest has occurred in 2-D layered transition-metal chalcogenide (TMC) nanocrystals as a consequence of their unique and exceptional mechanical, catalytic, optical, and electronic properties attributed to their layered structure and the presence of d-electrons of transition metals.[4] TMC nanocrystals are composed of highly anisotropic planar structure with van der Waals interactions between layers.[5] Such materials characteristics can also be complementary to what is lacking from graphene, e.g., changes from indirect to direct band gap and from metallic to semiconducting properties are possible, which is essential for energy harvesting applications.[4,6] Moreover, modulation of size, layer thickness, and composition can offer TMC materials a variety of unique properties, and in the cases for early TMCs, 2H $NbSe_2$ and 2H TaS_2 are superconductors with strong anisotropic in-plane metallic properties, and 1T TiS_2 is highly effective host material for Li ion with small lattice expansion.[6b,7]

The currently known preparatory protocols for generating TMC nanomaterials are shown in Scheme 1. A mechanical

Scheme 1. Schematic Illustration of 2-D Layered Nanomaterials[a]
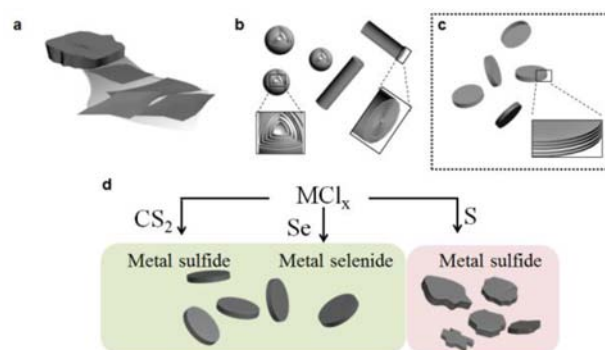
[a](a,b) Exfoliated nanosheets and closed 2-D materials by using mechanical exfoliation and high-temperature gas−solid method, respectively. (c) Free standing 2-D layered nanocrystals formed by using colloidal synthetic method. (d) Overall schematic route of 2-D layered nanocrystals obtained from different chalcogen precursors (CS_2, S, and Se). CS_2 and Se are suitable chalcogen precursors, while S is not a proper chalcogen precursor for the formation of TMCs (M = transition metals, x = 4 or 5).

exfoliation method is employed to prepare single or multilayers of nanosheets through peeling of bulk materials (Scheme 1a).[8] In addition, closed structural forms of quasi 0-D and 1-D nanotubes of layered TMCs are obtained by high temperature (>600 °C) solid−gas phase process (Scheme 1b).[9] Lastly, a solution-based colloidal synthetic route can be useful because it has advantages, such as mild reaction conditions and easy tunability in terms of size, composition, and monodispersity.[10] Unfortunately, current synthetic methodologies utilizing colloidal routes for formation of layered TMC nanocrystals in a rigorous nanoscale size regime (<100 nm) are rare and only provide partial synthetic information without systematic applicability on a variety of TMCs (Scheme 1c).[11] In this study, we demonstrate general and highly effective synthetic

protocols for all of the early transition-metal (group IV and V) chalcogenide (sulfide and selenide) nanocrystals via the reaction of metal chloride and carbon disulfide (CS_2) or elemental Se in the presence of oleylamine under mild conditions (Scheme 1d).

We introduce TiS_2 and $TiSe_2$ as representative cases to find out optimal synthetic conditions for 2-D layered TMC nanocrystals. Elemental S is selected as a chalcogen source since it has been widely utilized in the synthesis of metal sulfide nanocrystals of other dimensionality, such as spheres and rods.[12] We find that TiS_2 nanocrystals obtained by using elemental S are not satisfactory and in poor quality in terms of size, shape, and crystallinity according to TEM and XRD analyses (Figure S1). We discover that the generation of highly reactive radicals from elemental S during the reaction promotes degradation of the structural integrity of 2-D layered nano-crystals (vide infra). In order to avoid reactive radical formation, CS_2 is chosen as an alternative chalcogen precursor with a slight modification of previous report.[13] When $TiCl_4$ (2.0 mmol) and CS_2 (6.6 mmol) are reacted in oleylamine (11.2 mmol) at 300 °C, excellent quality TiS_2 nanocrystals are obtained via in situ generation of H_2S as an intermediate reactant (Figure 1a) (vide infra).[14] TEM analysis reveals that the obtained TiS_2 nanocrystal has a disc shape with a 100 nm lateral size and a 10 nm thickness with excellent crystallinity (Figure 1b,c). HRTEM image of the edge shows that a TiS_2 nanocrystal is composed of (001) layers with an interplanar spacing of 5.7 Å (Figure 1c). Each layer of TiS_2 comprises S–Ti–S triatomic layers corresponding to 1T–TiS_2 (Figure 1d).
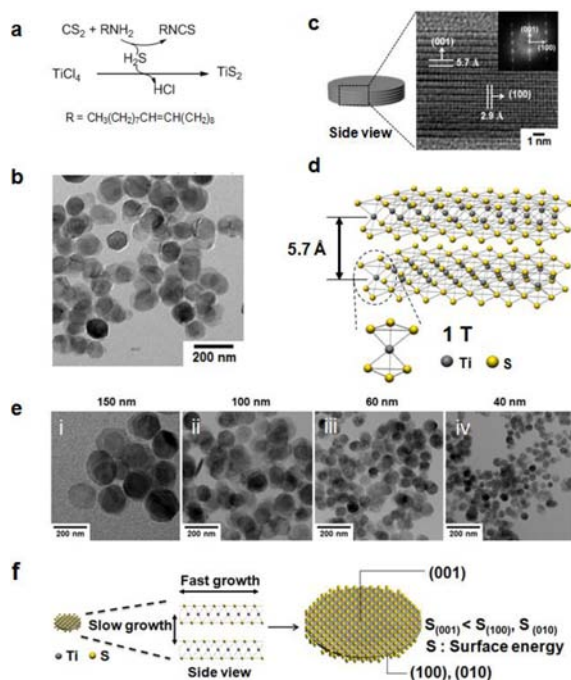
For 2-D layered nanostructures, both thickness and lateral size significantly affect materials properties, but so far most research has been focused on the thickness control via exfoliation techniques[4a,6a,8] with challenges on the lateral size control.[11a,15] Consequently, it is significant that the methodology described above can be readily used to control the lateral size of TiS_2 nanocrystals by adjusting reactant concentration (Figures 1e and S1B).[16] One of the reasons of such an anisotropic growth is the large difference of surface energies of 1T layered nanostructures, including TiS_2 where (100) and (010) surfaces exhibit higher surface energy than that of (001) surfaces (Figure 1f).[16b] A described synthetic method of TiS_2 nanocrystal is readily applicable to other group V and IV transition-metal sulfide nanocrystals such as VS_2, NbS_2, TaS_2, ZrS_2,[11a] and HfS_2 (Figures 2 and S2 and details in SI).
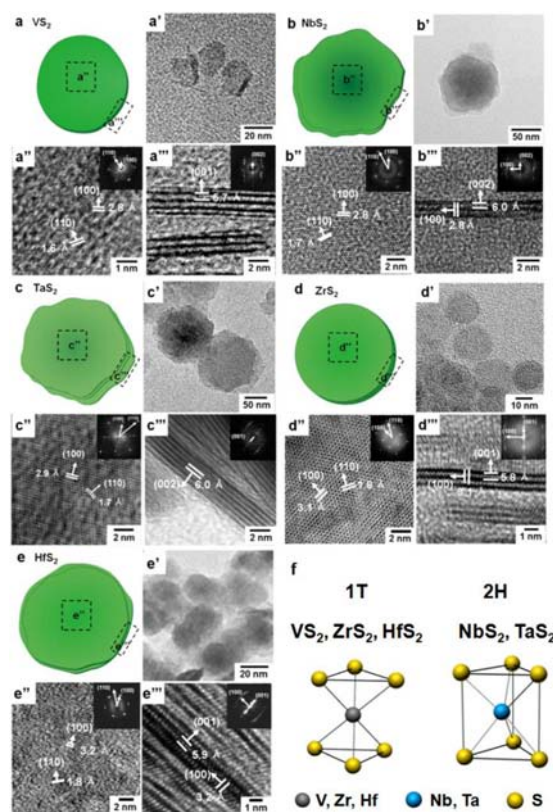

Figure 2. Generalized synthesis of group V and IV transition-metal sulfide nanocrystals. (a–e) Illustration of shape of 2-D layered metal sulfide nanocrystals. TEM images of (a′) VS_2 (18 ± 2.2 nm), (b′) NbS_2 (100 ± 30 nm), (c′) TaS_2 (120 ± 23 nm), (d′) ZrS_2 (20 ± 2.1 nm), and (e′) HfS_2 (20 ± 2.8 nm). (a″–e″) Top and (a‴–e‴) side-view HRTEM images of metal sulfide nanocrystals. (f) Schematic illustration of 1T (VS_2, ZrS_2, and HfS_2) and 2H (NbS_2 and TaS_2) structures.

Figure 1. Synthesis of TiS_2 nanocrystals. (a) Chemical reactions for TiS_2. (b) Low-magnification TEM image. (c) Side-view HRTEM image and FFT patterns (inset) of a TiS_2 nanocrystal. (d) Visualization of TiS_2 using a ball and stick model to illustrate the 2-D layered nanocrystal composed of trigonal structure (1T) (gray, titanium; yellow, sulfur). (e) Size-controlled synthesis of TiS_2 nanocrystals: (i–iv) TEM images with different lateral sizes: (i) 150 ($\sigma \approx 13\%$), (ii) 100 ($\sigma \approx 14\%$), (iii) 60 ($\sigma \approx 14\%$), and (iv) 40 nm ($\sigma \approx 17\%$). (f) Schematic illustration of anisotropic growth.

In contrast with problems associated with the use of elemental S in the synthesis of metal sulfides, elemental Se can be employed to prepare group IV and V metal selenide nanocrystals. The reason for this resides in the fact that the elemental Se generates relatively mild radical species compared to its S counterpart (vide infra). In addition, other potential Se precursors, such as CSe_2, are not suitable due to high toxicity and poor stability.[17] In fact, a previous report shows that elemental Se can be an effective source for $NbSe_2$.[11b] The reaction scheme used for generation of the $TiSe_2$ nanocrystals is

displayed in Figure 3a. TEM analysis shows TiSe$_2$ nanocrystals having a lateral size of 250 nm ($\sigma \approx 29\%$) and a thickness of 30
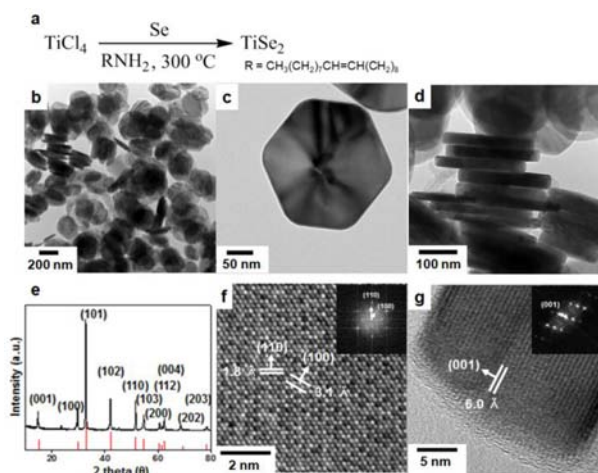

Figure 3. Synthetic protocol of TiSe$_2$ nanocrystals. (a) Reaction equation. (b,d) Low-magnification TEM images. (c) Top view of a TiSe$_2$ nanocrystal. (e) XRD patterns of TiSe$_2$ nanocrystals (JCPDS 301383). (f) Top- and (g) side-view HRTEM images and FFT patterns (inset) of a TiSe$_2$ nanocrystal.

nm ($\sigma \approx 7\%$) (Figure 3b−d). XRD patterns correspond to hexagonal structure of $P\bar{3}m1$ 1T-type TiSe$_2$ (Figure 3e). HRTEM images contain lattice fringes of 1.8, 3.1, and 6.0 Å for the (110), (100), and (001) planes, respectively (Figure 3f,g). In addition, regular hexagonal patterns seen in the FFT of HRTEM lattice images indicate a single crystallinity of TiSe$_2$ nanocrystal (Figure 3f,g inset). This protocol for TiSe$_2$ nanocrystal is successfully extended to other group IV and V transition-metal selenide nanocrystals, including ZrSe$_3$, HfSe$_3$, VSe$_2$, NbSe$_2$, and TaSe$_2$ (Figures S3,S4 and details in SI).

The results summarized above demonstrate that appropriate chalcogen precursor is critical in order to carry out successful synthesis of 2-D layered TMC nanocrystals. Although elemental S has been used for the synthesis of various metal sulfide nanocrystals, it is inappropriate to the generation of 2-D layered metal sulfide nanocrystals. In contrast, the use of elemental Se is quite effective for the formation of high-quality 2-D layered TMC nanocrystals. In an electron paramagnetic resonance (EPR) study, we observe that heating elemental S and Se in oleylamine leads to production of radical species. In contrast, no radical species are formed when CS$_2$ in oleylamine is heated (Figure 4a). We explore the effects of radicals on the stability of 2-D layered TMC nanocrystals. When exposed to highly reactive radical species, azobisisobutyronitrile (AIBN) at 300 °C, the structural degradation of TiS$_2$ and TiSe$_2$ is clearly observed (Figures 4b and S5). Similar to AIBN, sulfur radicals also promote degradation of TiS$_2$ nanocrystals, and Figure 4c obviously shows the degradation of a TiS$_2$ nanocrystal in time-dependent manner. When AIBN is incorporated during the TiS$_2$ growth from CS$_2$ precursor, the degradation of TiS$_2$ nanocrystals is also effective. As reaction time passes from 10 to 20 and 50 min, the size distribution of TiS$_2$ nanocrystals becomes broader compared to the case when AIBN is absent (Figure 4d). This phenomenon is presumably a consequence of simultaneous nanocrystal growth and degradation.

Similar to TiS$_2$ nanocrystals, the significant degradation is shown in TiSe$_2$ nanocrystals with the treatment of elemental S
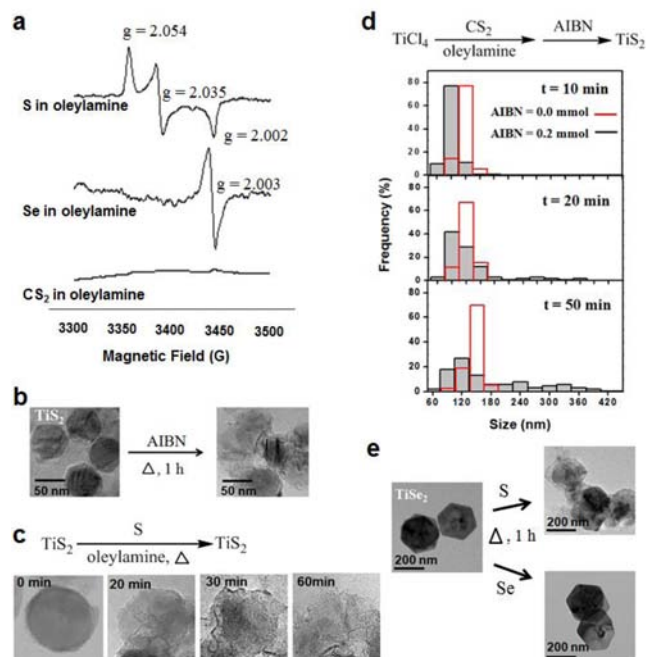

Figure 4. (a) EPR spectra of elemental S and Se and CS$_2$ in oleylamine measured at 9.6 GHz (60 K). No EPR signal is detected in an oleylamine solution of CS$_2$. (b) TEM images of TiS$_2$ nanocrystals treated with AIBN (0.5 mmol) in oleylamine at 300 °C. (c) Time-dependent morphology changes associated with degradation of TiS$_2$ nanocrystals treated with elemental S (0.5 mmol) at 300 °C at 0, 20, 30, and 60 min. (d) Radical (AIBN) effects on TiS$_2$ nanocrystals during growth processes. Size distribution histograms of TiS$_2$ nanocrystals at 10, 20, and 50 min in the absence (red column) and presence (gray column) of AIBN. (e) TEM images of TiSe$_2$ nanocrystals treated with elemental S (0.5 mmol) and Se (0.5 mmol) in oleylamine at 300 °C.

(0.5 mmol) at 300 °C (Figure 4e). However, no noticeable change takes place when these nanocrystals are exposed to elemental Se treatment (Figure 4e). These observations are consistent with the reactivity differences of S and Se radicals, where S radicals are known to be much more reactive.[18] Thus, highly reactive radicals arising from elemental S and AIBN cause degradation of layered nanocrystals, but relatively less reactive radicals generated from elemental Se do not adversely impact the formation of high-quality metal selenide nanocrystals. Our observation is presumably due to the unique structural features of 2-D layered materials with open peripheral edges and easy internal accessibility of reactive radical species via weak bonding between the layers.[19] In contrast, no structural degradation for closely packed solid structures, such as zinc blende nanocrystals, is observed even in the presence reactive radical species (Figure S6).

In conclusion, we have shown that general synthetic protocols are possible for 2-D layered early transition-metal sulfide and selenide nanocrystals. The group IV and V metal sulfide and selenide nanocrystals prepared in this effort have highly crystalline, well-defined layered structures with lateral sizes that are <200 nm. In addition, our findings propose that the use of appropriate chalcogen precursors is critical component of the strategies, where CS$_2$ is more suitable for the formation of metal sulfide nanocrystals, while elemental Se is proper for the generation of metal selenide nanocrystals. Considering the fact that interest in 2-D layered TMC

nanocrystals has become intense, the findings from our investigation here may serve as an important guide for the synthesis of various kinds of 2-D layered TMC nanocrystals.[11]

■ ASSOCIATED CONTENT

Ⓢ Supporting Information

Detailed synthetic methods and X-ray diffraction patterns. This material is available free of charge via the Internet at http://pubs.acs.org.

■ AUTHOR INFORMATION

Corresponding Author

jcheon@yonsei.ac.kr

Author Contributions

[†]These authors contributed equally.

Notes

The authors declare no competing financial interest.

■ ACKNOWLEDGMENTS

■ REFERENCES

(1) (a) Kan, S.; Mokari, T.; Rothenberg, E.; Banin, U. *Nat. Mater.* **2003**, *2*, 155−158. (b) Burda, C.; Chen, X.; Narayanan, R.; El-Sayed, M. A. *Chem. Rev.* **2005**, *105*, 1025−1102. (c) Zhuang, Z.; Peng, Q.; Li, Y. *Chem. Soc. Rev.* **2011**, *40*, 5492−5513. (d) Pacholski, C.; Kornowski, A.; Weller, H. *Angew. Chem. Int. Ed.* **2002**, *41*, 1188−1191. (e) Shenhar, R.; Norsten, T. B.; Rotello, V. M. *Adv. Mater.* **2005**, *17*, 657−669.

(2) (a) Xia, Y.; Yang, P.; Sun, Y.; Wu, Y.; Mayers, B.; Gates, B.; Yin, Y.; Kim, F.; Yan, H. *Adv. Mater.* **2003**, *15*, 353−389. (b) Cozzoli, P. D.; Pellegrino, T.; Manna, L. *Chem. Soc. Rev.* **2006**, *35*, 1195−1208. (c) Zhai, T.; Li, L.; Ma, Y.; Liao, M.; Wang, X.; Fang, X.; Yao, J.; Bando, Y.; Golberga, D. *Chem. Soc. Rev.* **2011**, *40*, 2986−3004. (d) Alivisatos, P. *Pure Appl. Chem.* **2000**, *72*, 3−9.

(3) (a) Prasad, S; Zabinski, J. *Nature* **1997**, *387*, 761−763. (b) Ithurria, S.; Tessier, M.; Mahler, B.; Lobo, R. P. S. M.; Dubertret, B.; Efros, A. *Nat. Mater.* **2011**, *10*, 936−941. (c) Kong, D.; Chen, Y.; Cha, J.; Zhang, Q.; Analytis, J.; Lai, K.; Liu, Z.; Hong, S.; Koski, K. J.; Mo, S.; Hussain, Z.; Fisher, I.; Shen, Z.-X.; Cui, Y. *Nat. Nanotechnol.* **2011**, *6*, 705−709. (d) Cho, S.; Butch, N. P.; Paglione, J.; Fuhrer, M. S. *Nano Lett.* **2011**, *11*, 1925−1927.

(4) (a) Radisavljevic, B.; Radenovic, A.; Brivio, J.; Giacometti, V.; Kis, A. *Nat. Nanotechnol.* **2011**, *6*, 147−150. (b) Lee, C.; Li, Q.; Kalb, W.; Liu, X.; Berger, H.; Carpick, R. W.; Hone, J. *Science* **2010**, *328*, 76−80. (c) Jaramillo, T. F.; Jørgensen, K. P.; Bonde, J.; Nielsen, J.; Horch, S.; Chorkendorff, I. *Science* **2007**, *317*, 100−102. (d) Johari, P.; Shenoy, V. *ACS Nano* **2012**, *6*, 5449−5456. (e) Eda, G.; Yamaguchi, H.; Voiry, D.; Fujita, T.; Chen, M.; Chhowalla, M. *Nano Lett.* **2011**, *11*, 5111−5116.

(5) (a) Wilson, J. A.; Yoffe, A. D. *Adv. Phys.* **1969**, *18*, 193−335. (b) Dresselhaus, M. S. *Intercalation in Layered Materials*; NATO ASI Series; Plenum Press: New York, 1986. (c) Chen, J.; Tao, Z.-D.; Li, S.-L. *Angew. Chem., Int. Ed.* **2003**, *42*, 2147−2151. (d) Chhowalla, M.; Amaratunga, G. A. J. *Nature* **2000**, *407*, 164−167.

(6) (a) Splendiani, A.; Sun, L.; Zhang, Y.; Li, T.; Kim, J.; Chim, C.-Y.; Galli, G.; Wang, F. *Nano Lett.* **2010**, *10*, 1271−1275. (b) Winter, M.; Besenhard, J.; Spahr, M. E.; Novák, P. *Adv. Mater.* **1998**, *10*, 725−763.

(7) (a) Edwards, J.; Frindt, R. F. *J. Phys. Chem. Solids* **1971**, *32*, 2217−2221. (b) Frindt, R.; Murray, R.; Pitt, G.; Yoffe, A. *J. Phys. C* **1972**, *5*, 154−156.

(8) Smith, R. J.; King, P. J.; Lotya, M.; Wirtz, C.; Khan, U.; De, S.; O'Neill, A.; Duesberg, G. S.; Grunlan, J. C.; Moriarty, G.; Chen, J.; Wang, J.; Minett, A. I.; Nicolosi, V.; Coleman, J. N. *Adv. Mater.* **2011**, *23*, 3944−3948.

(9) (a) Tenne, R. *Nat. Nanotechnol.* **2006**, *1*, 103−111. (b) Nath, M.; Rao, C. N. R. *Angew. Chem., Int. Ed.* **2002**, *41*, 3451−3454. (c) Parilla, P. A.; Dillon, A. C.; Jones, K. M.; Riker, G.; Schulz, D. L.; Ginley, D. S.; Heben, M. J. *Nature* **1999**, *397*, 114.

(10) (a) Puntes, V. F.; Krishnan, K. M.; Alivisatos, A. P. *Science* **2001**, *291*, 2115−2117. (b) Yin, Y.; Alivisatos, A. P. *Nature* **2005**, *437*, 664−670. (c) El-Sayed, M. A. *Acc. Chem. Res.* **2004**, *37*, 326−333.

(11) (a) Jang, J.-t.; Jeong, S.; Seo, J.-w.; Kim, M.-c.; Sim, E.; Oh, Y.; Nam, S.; Park, B.; Cheon, J. *J. Am. Soc. Chem.* **2011**, *133*, 7636−7639. (b) Sekar, P.; Greyson, E. C.; Barton, J. E.; Odom, T. W. *J. Am. Chem. Soc.* **2005**, *127*, 2054−2055. (c) Park, K. H.; Choi, J.; Kim, H. J.; Oh, D.-H.; Ahn, J. R.; Son, S. U. *Small* **2008**, *4*, 945−950.

(12) (a) Li, L. S.; Pradhan, N.; Wang, Y.; Peng, X. *Nano Lett.* **2004**, *4*, 2261−2264. (b) Jun, Y.; Lee, S.; Kang, N.-J.; Cheon, J. *J. Am .Chem. Soc.* **2001**, *123*, 5150−5151. (c) Joo, J.; Na, H. B.; Yu, T.; Yu, J. H.; Kim., Y. W.; Wu, F.; Zhang, J. Z.; Hyeon, T. *J. Am. Chem. Soc.* **2003**, *125*, 11100−11105.

(13) Jeong, S.; Han, J. H.; Jang, J.-t.; Seo, J.-w.; Kim, J.-G.; Cheon, J. *J. Am. Chem. Soc.* **2011**, *133*, 14500−14503.

(14) Ballabeni, M.; Ballini, R.; Bigi, F.; Maggi, R.; Parrini, M.; Predieri, G.; Sartori, G. *J. Org. Chem.* **1999**, *64*, 1029−1032.

(15) Wilcoxon, J. P.; Samara, G. A. *Phy. Rev. B* **1995**, *51*, 7299−7302.

(16) (a) Shevchenko, E. V.; Talapin, D.; Schnablegger, H.; Kornowski, A.; Festin, Ö.; Svedlindh, P.; Haase, M.; Weller, H. *J. Am. Chem. Soc.* **2003**, *125*, 9090−9101. (b) According to ab initio calculations of surface energies (S) of TiS_2 nanocrystals, edge facets such as (100) or (010) [$S_{(100), (010)}$ = 55.8 meV/Å^2] show larger surface energies than basal (001) plane [$S_{(001)}$ = 12.5 meV/Å^2]

(17) Wudl, F. Process for producing chalcogen containing compounds. U.S. Patent 4,462,938, July 31, 1984.

(18) (a) Tsuchii, K.; Tsuboi, Y.; Kawaguchi, S.-I.; Takahashi, J.; Sonoda, N.; Nomoto, A.; Ogawa, A. *J. Org. Chem.* **2007**, *72*, 415−423. (b) Yordanov, G. G.; Yoshimura, H.; Dushkin, C. D. *Colloid Polym. Sci.* **2008**, *286*, 813−817.

(19) (a) Jung, M.; Handa, H.; Takahashi, R.; Fukidome, H.; Suemitsu, T.; Otsuji, T.; Suemitsu, M. *Jpn. J. Appl. Phys.* **2011**, *50*, 070107−1−5. (b) Zaldivar, R. J.; Adams, P. M.; Nokes, J.; Kim, H. I. *J. Vac. Sci. Technol. B* **2012**, *30*, 03D107−1−7.